# Variations of the Argentine Gyre Observed in the GRACE Time-Variable Gravity and Ocean Altimetry Measurements

**Y. Yao[1,2], B. F. Chao[2]*, D. García-García[3], and Z. Luo[4]**

[1] School of Geodesy and Geomatics, Wuhan University, Wuhan, China

[2] Institute of Earth Sciences, Academia Sinica, Taipei, Taiwan

[3] Applied Mathematics Department, University of Alicante, Alicante, Spain

[4] MOE Key Laboratory of Fundamental Physical Quantities Measurement, School of Physics, Huazhong University of Science and Technology, Wuhan, China

*Corresponding author: Benjamin F. Chao (bfchao@earth.sinica.edu.tw)

**Key Points:**

- GRACE gravity data agree well with altimetry confirming the barotropic nature of a ~25-day oscillation within the Argentine Gyre.
- The Argentine Gyre undulates up-and-down in sea level variation in pace with Antarctic Oscillation temporally.
- GRACE observes oceanographic signals not contained in de-aliasing ocean model at temporal resolutions higher than practiced hitherto.



This article has been accepted for publication and undergone full peer review but has not been through the copyediting, typesetting, pagination and proofreading process which may lead to differences between this version and the Version of Record. Please cite this article as doi: 10.1029/2018JC014189

**Abstract**

We investigate the non-seasonal and high-frequency variations of the Argentine Gyre in the south Atlantic Ocean by analyzing the time-variable gravity (TVG) measurements from the GRACE satellite mission in conjunction with the satellite ocean altimetry and two ocean general circulation model outputs (GLORYS2V4 and ECCO V4R3). We solve the empirical orthogonal functions (EOF) and complex EOF (CEOF), and find good agreement between TVG and altimetry observations, confirming the barotropic structure of the Argentine Gyre. In particular, the leading EOF modes of the overall up-and-down undulation in TVG and altimetry variations are found to be in pace temporally with the Antarctic Oscillation Index with correlation as high as 0.69 at zero time shift. Furthermore, the leading CEOF mode signifies a counterclockwise dipole pattern of ~25-day periodicity within the overall gyre with multi-scale amplitude modulation. The fact that GRACE does observe these signals, while the de-aliasing background ocean model fails to, ascertains that GRACE data have adequate sensitivity to allow the detection of TVG signals at spatial and temporal resolutions higher than practiced hitherto. The ~25-day oscillation is well recovered in the GLORYS2V4 ocean general circulation model, but not in ECCO V4R3. Our study demonstrates that satellite-observed TVG fields can be useful in studying oceanographic gyres, particularly the polar gyres, that are not well-observed by altimetry and in situ data.

**Plain Language Summary**

The Argentine Gyre is a persistent, energetic mesoscale circulation in the south Atlantic Ocean. We study its non-seasonal variability by analyzing data from the satellite mission GRACE that measures the time-variable gravity, in conjunction with the ocean altimetry and two ocean general circulation model outputs. We find good matching of the overall strength of the gyre with the Antarctic Oscillation in the Southern Hemisphere. We also confirm the existence of a high-frequency rotary oscillation within the gyre at ~25-day periodicity. We demonstrate that GRACE is sensitive enough to detect oceanographic signals at spatial and temporal resolutions higher than practiced hitherto.

## 1 Introduction

The Argentine Basin in the south Atlantic Ocean is a region of complex oceanographic variability of a wide range of temporal and spatial scales (Fu, 2007). Within the region located over the Zapiola Rise, which is a sediment deposit ~1000 m above the abyssal plain of over 5 km in depth (Saraceno et al., 2009), the energetic Argentine Gyre (also known as the Zapiola anticyclone) is a high pressure system circulating counterclockwise under the geostrophic balance between the outward pressure gradient force and the inward Coriolis force (to the left of the flow direction in the Southern Hemisphere) (Figure 1). The Argentine Gyre extends about 1000 km in the zonal and 500 km in the meridional directions, with a transport of more than 80 Sv (1 Sv = $10^6$ $m^3s^{-1}$) (Artana et al., 2016; Hughes et al., 2007; Saraceno et al., 2012; Saunders & King, 1995), comparable to major surface oceanic streams. It is associated with a local minimum in eddy kinetic energy, isolated by closed planetary contours of potential vorticity $f/h$ (Saraceno et al., 2012), where $f$ is the planetary vorticity or Coriolis parameter, and $h$ the water depth. To the west, the equatorward flowing Malvinas Current, an offshoot of the mighty Antarctic Circumpolar Current (ACC, with a mean flux of 137 ±7 Sv, Meredith et al., 2011), collides with the poleward flowing Brazil Current at about 38°S, forming the Brazil/Malvinas Confluence (BMC) that is one of the most energetic regions of the world ocean (Hughes et al., 2007; Saraceno et al., 2004). Two major fronts of ACC, the Subantarctic Front and Polar Front flow eastward in the south of the Argentine Basin.

Believed to have existed for upwards of many millennia (Flood & Shor, 1988), the Argentine Gyre has only been revealed by modern observations rather recently (Flood & Shor, 1988; Saunders & King, 1995; Weatherly, 1993). The Argentine Gyre is poised to have a profound impact on the heat exchange between the Southern Ocean and lower latitudes (de Miranda et al., 2011) and South Atlantic's inter-ocean exchanges (Garzoli et al., 2008). The

variability of the Argentine Gyre ranges from hours to interannual periods in timescale and has been studied using in situ measurements from ocean bottom current meters (Weatherly et al., 1993) and pressure gauges (Hughes et al., 2007), satellite ocean altimetry (Fu et al., 2001; Saraceno et al., 2009), as well as numerical models (Bigorre et al., 2009; Venaille et al., 2011). In particular, a dominant and consistent mode of ~25-day barotropic counterclockwise oscillation has been reported, where Fu et al. (2001), Tai and Fu (2005) and Weijer et al. (2007) have demonstrated that the satellite altimetry proves to be effective in giving a fairly complete description of the ~25-day oscillation of the Argentine Gyre.

In this paper we investigate the non-seasonal and particularly the ~25-day sea level variations (SLV) of the Argentine Gyre, using time-variable gravity (TVG) data from the Gravity Recovery and Climate Experiment (GRACE) satellite mission in conjunction with ocean altimetry data, and the GLORYS2V4 and Estimating the Circulation and Climate of the Ocean version 4 release 3 (ECCO V4R3) ocean general circulation model outputs (OGCMs). Since its launch in 2002, GRACE has provided the TVG field of the Earth as monthly global products (Tapley et al., 2004). The TVG caused by Argentine Gyre's strong SLV of up to 20 cm covering the spatial range of more than 500 km is significantly above the GRACE detectability level. As far as GRACE is concerned, the issue then is whether the temporal resolution of GRACE data is sufficient to allow detailed studies. The TVG at a ~25-day period cannot be resolved in the GRACE monthly solutions which would produce aliased patterns (Hughes et al., 2007). However, thanks to the continual improvements in the GRACE data quality, 10-day-resolution TVG product (GRGS RL03 10-day solutions, courtesy of the Group de Research de Geodesie Spatiale) with the Nyquist period of 20 days, has become available, making the detection of ~25-day signal possible in principle. We mean to "push the envelope" to demonstrate GRACE's capability in capturing clearly the TVG signals of small spatial scale and short time scale, as exemplified by the Argentine Gyre. We

shall investigate the non-seasonal, broad-band variations of the Argentine Gyre by the empirical orthogonal function (EOF) method (e.g., Hannachi et al., 2007; Preisendorfer & Mobley, 1988), and revisit the ~25-day oscillation within the Argentine Gyre by the application of the complex EOF (CEOF) (e.g., Hannachi et al., 2007; see also Fu et al., 2001).

The physical mechanisms responsible for the persistence and variability of the Argentine Gyre are inadequately known, yet generally accepted to be associated with the interaction of mesoscale eddies with seafloor topography (Dewar et al., 1998). Hughes et al. (2007) elaborated on the physical mechanism that the signals in the Argentine Basin are related to topographically steered resonant barotropic modes energized by interactions between the mean flow of the ACC (and adjacent current systems) and the local mesoscale Eddy field. We will not attend much to the mesoscale eddies in this study because their spatial scale in the range of 50-200 km is not resolvable by GRACE, whereas satellite altimetry has proven to be effective in tracking eddies (Isern-Fontanet et al, 2003; Chelton et al., 2011).

The Antarctic Oscillation (AAO), also known as the Southern Annular Mode, is the principal mode of atmospheric variability in the Southern Hemisphere (Marshall, 2003). The strength of AAO is customarily quantified by the AAO Index, defined as the leading principal component of the 700 hPa atmospheric geopotential height anomalies poleward of 20°S (Mo, 2000). Believed to be a distinctive source of large-scale variability in the Southern Ocean, AAO can be expected to have a direct influence on the variability of the Argentine Gyre, which we shall examine numerically by analyzing their cross correlations.

Two facts should be recognized at the outset. Firstly, the observed SLV, say by ocean altimetry, manifests the combined effects of the steric effect of temperature and salinity changes plus the mass redistribution, the latter constitutes what is detectable by GRACE (Cazenave & Nerem, 2004). In our case we compare directly the GRACE and altimetry

measurements below on the account that the non-seasonal variations of the Argentine Gyre are mainly mass-induced and that the associated steric effect is negligible (Hughes et al., 2007; Saraceno et al., 2009; Volkov & Fu, 2008). Secondly, what we study here is the *variation* of the Argentine Gyre and not the gyre itself, since GRACE's TVG signal, as the nomenclature suggests, sees the variation relative to the mean gravity field or sea level. This is also true for the altimetry data, which depicts the sea level changes in reference to a time-averaging field, in our case the 1993-2012 Mean Dynamic Topography.

## 2 Data Processing and Analysis

### 2.1 TVG data from GRACE

We adopt the GRACE GRGS RL03 10-day solutions for the Argentine Gyre region (Figure 1) spanning the 10-year period from 2003/1/5 to 2013/1/1 (data after year 2012 are beset with numerous drop-outs and hence not used). The solutions are given in spherical harmonic coefficient anomalies up to degree and order 80, with a spatial resolution of ~300 km for the Argentine Basin latitudes. The main GRACE product is the GRACE-observed TVG solved upon the removal of the GAA and GAB products for de-aliasing purposes; the latter two give the non-tidal variations of atmospheric and ocean mass calculated from the respective atmospheric and oceanic general circulation models. For our present oceanographic study, we add back the GAB to restore the "full" ocean mass variations as suggested by Dobslaw et al. (2017). The inverted-barometer effect is to be corrected to make the mass-induced sea level variations from GRACE comparable with altimetric SLV. To make this correction, we simply take GAA minus its area-mean averaged over the global ocean area to get the local atmospheric mass anomalies, which are added back to the oceanic mass variations (García-García et al., 2010; Willis et al., 2008). As is common practice, the

degree 0 and 1 terms are set to zero, and the $C_{20}$ coefficients replaced by those from the satellite laser ranging technique (Cheng et al., 2011). No extra smoothing or filtering is applied since the 10-day GRACE dataset used here has already been stabilized during its generation processing. The oceanic areas within ~3° off the South America coast are excluded from our analysis below to avoid signal leakages from land hydrology, which are typically larger than oceanic signals.

We assume that the TVG signals are produced physically by mass transports that only occur on the Earth surface, a supposition that is ensured as we shall remove empirically the secular terms from the data so that any tectonic and glacial isostatic adjustment signals will be excluded. Under that assumption, we can convert the GRACE TVG solutions directly to the equivalent (salt) water thickness (salt water density of 1028 kg/m$^3$ is used in this study; Chao et al., 1987; Chao, 2005; Wahr et al., 1998), or the SLV in the present case. We then least-squares fit and subtract from our GRACE SLV the mean, the trend, and the annual and semi-annual sinusoidal terms. The residual, i.e., the non-seasonal broad-band SLV, are fed into the EOF scheme to analyze the standing oscillations of the Argentine Gyre. We normalize the spatial pattern of the EOF w.r.t. its standard deviation, so the corresponding time series manifests the actual amplitude of the SLV, here in unit of centimeter (cm).

On the other hand, the high-frequency propagating waves within the gyre, here the ~25-day oscillation, are better captured by the CEOF method within a relatively narrow frequency band. In the latter case the above non-seasonal SLV are high-pass filtered at the cutoff period of 30 days and subsequently subjected to the CEOF analysis. We expect to see in the CEOF modes the circularly propagating feature of the ~25-day oscillation manifested by the spatial and corresponding temporal phasing, as well as its amplitude variabilities.

On the other side, we also test another GRACE TVG solution dataset, namely the ITSG-Grace 2016 daily solutions up to degree 40 ( Mayer-Gürr et al., 2016) for 2013/1/21-

2014/3/19 with the actual temporal sampling in the range of 2-4 days. We shall apply the same processing as above to search for the ~25-day oscillation in the Argentine Basin.

## 2.2 Altimetric SLV data

We do our GRACE analysis in conjunction with satellite ocean altimetry data which have proved to be effective in delineating Argentine Gyre's ~25-day oscillation (Fu et al., 2001; Tai & Fu, 2005; Weijer et al., 2007). We take the daily maps of Absolute Dynamic Topography (courtesy of CMEMS) derived from multiple-satellite altimetry observations for the 23-year long period of 1993-2015. The data are given on a 0.25° × 0.25° latitude/longitude grid, with a temporal resolution of better than 10 days. Tides and the inverted-barometer effect have been removed during processing.

We subtract out the Mean Dynamic Topography referenced to the period 1993-2012 from the above to obtain the altimetric SLV. To reduce the signature of the eddies, we apply a Gaussian weighted spatial filter, where the search window has a dimension of 3° × 6°, and the half-weight scale is set to 1.5° in latitude and 3° in longitude, matching the spatial resolution of the filtered altimetric SLV to that of the GRACE SLV. The filtered altimetric SLV are then put through the similar processing as to the GRACE SLV to obtain the non-seasonal SLV and its subsequent high-frequency version, which are then likewise subjected to the EOF and the CEOF analysis respectively as above.

## 2.3 Ancillary OGCMs

Output data from two OGCMs are considered here to help assess the discrepancies between satellite altimetry and GRACE results. The first is the GLORYS2V4 global ocean reanalysis, which assimilates the observations from satellite altimetry, in situ profiles of

temperature and salinity, sea surface temperature, and sea ice concentration. It describes the mean and time-variable state of the ocean circulation including a part of the mesoscale eddy field. We use its daily sea surface height output given on a 0.25° × 0.25° latitude/longitude grid, spannig the period of 1993/1/1-2015/12/29.

The second is the ECCO V4R3 product that synthesizes the MIT GCM as well as satellite and in situ data including those from satellite altimetry, in situ profiles of temperature and salinity, GRACE and Aquarius observations (Fukumori et al., 2017), and focuses on large-scale variabilities (of spatial resolutions larger than 3-grid points). The ECCO V4R3 sea surface heights are given on an uneven grid (around 0.7° × 1° latitude/longitude in the Argentine Basin) with daily sampling covering the time-span of 1992-2015.

We apply the same numerical processing as described in Section 2.2 to both the GLORYS2V4 and ECCO V4R3 sea surface heights and obtain the leading EOF and CEOF modes. The spatial Gaussian smoothing is not required for ECCO V4R3 data, as the spatial resolution of ECCO V4R3 does not allow representation for the eddy fields.

## 3 Results

### 3.1 Non-seasonal variations

Figure 2 presents the leading EOF mode of the non-seasonal SLV in the Argentine Basin from GRACE (GRACE EOF-1, explaining 29% of the total variance) and altimetry (Altimetry EOF-1, explaining 23% of the total variance). For Argentine Gyre that is a high-pressure system, a positive sea level anomaly means increased pressure gradient force to be counter-balanced by an increased Coriolis force, hence a faster spin. Figures 2a and 2b show their respective spatial patterns, which are in high resemblance. They exhibit the spatially

unison pattern (of essentially the same sign or polarity) relative to the mean state (which has been removed) expected of an entire gyre anomaly, which executes up-and-down undulations in SLV according to the corresponding time series. The slight difference in the northwest portion may be a result of the TVG signal leakage in the GRACE observation from the energetic BMC region.

The leading EOF time series in Figure 2c, the longer-timespan one for Altimetry EOF-1 and the shorter one GRACE EOF-1, indicate the spinning strength of the geostrophic Argentine Gyre as a whole: the gyre spins up when the sea level anomaly is positive and spins down when negative. Immediately one sees the agreement between the two time series, not only in the variability but also in their absolute amplitudes in cm, which are somewhat reduced from the true amplitude after the (identical) filtering process. This means that GRACE indeed captures well the structure and behavior of the Argentine Gyre in its entirety, and that its variation is barotropic in nature in both GRACE-derived and altimetric SLA. A linear correlation coefficient of 0.69 at zero time shift is found between the two time series of the leading EOF modes (see Figure 4b below), far exceeding the 99% confidence level of 0.14 in the case of our broad-band data of statistical degree of freedom of approximately 350.

Figures 2d and 2e present the (Morlet) wavelet time-frequency spectra (cf. Chao et al. 2014; Morlet et al. 1982) that we calculate for the said two time series. Interesting is the existence of a ~6-year periodicity, which is indicative of the interannual variability (of ~6-7 years) that could be set off by the basin mode perturbations in the Argentine Basin as suggested by Bigorre (2005) based on numerical simulations. A distinct and consistent quasi-biennial signal is also revealed in the wavelet spectra, whose origin is indeterminate presently. Our study suggests, though, that this is the circulating period of the Argentine Gyre's main flow, which we shall discuss later. There is a consistent ~160-day signal in the GRACE EOF-1 time series but absent in altimetry, presumably due to the aliasing from either

errors in the $S_2$ tide model or systemic effect in GRACE instrumentation (Cheng & Ries, 2017).

The curl of the velocity, known as the relative vorticity (as opposed to the planetary vorticity), describes the local spinning under the combined effects of curvature and shear of currents in the ocean. Assuming a pure geostrophic horizontal flow, the Argentine Gyre's relative vorticity (variation) $\xi$ in the vertical direction is a scalar proportional to the Laplacian of sea level (variation) *h*:

$$\xi = \frac{g}{f}\left(\frac{\partial^2 h}{\partial x^2} + \frac{\partial^2 h}{\partial y^2}\right) \quad (1)$$

where $g$ = 9.81 $ms^{-2}$ is the mean gravitational acceleration, $f$ = 2ωsin(latitude) is the Coriolis parameter or planetary vorticity (where $\omega = 7.292\times10^{-5} s^{-1}$ is the Earth's angular rotation rate). We have tried to calculate the $\xi$ directly from the altimetry and GRACE-derived non-seasonal SLV by Equation (1). However, the greatly amplified noises as a result of the double gradient, and hence their heightened weighting into the EOF processing, much hindered the EOF in extracting the coherent signals. Thus we alternatively take the spatial pattern of the leading EOF obtained in Figures 2a and 2b above to calculate the corresponding $\xi$ change (while the corresponding time series remain the same as Figure 2c of course) for the Argentine Gyre.

Figure 3 shows that the derived $\xi$ undergoes cyclonic and anticyclonic deviations from the mean circulation. The GRACE-derived result is uniform in the center of the Argentine Gyre (36°W-47°W, 43°S-47°S), while the altimetry-derived gives more details: the $\xi$ in the center of Zapiola Drift (43°W, 45°S) barely changes. When the Argentine Gyre goes up in

SLA as in Figures 2a and 2b, it spins faster with positive $\xi$ change as shown in the center of Figures 3a and 3b. Regions surrounding the anticyclonic center have different vorticity polarities mainly along the zonal direction as a consequence of the conservation of *f/h*.

3.2 AAO connections

We study the correlation of the non-seasonal variation of the Argentine Gyre, represented by the time series of GRACE EOF-1 and Altimetry EOF-1, with the AAO represented by the daily AAO Index (courtesy of USA National Oceanic and Atmospheric Administration). We low-pass filter the three time series to period range longer than 200 days. They are displayed in Figure 4a.

Figures 4b-d show the cross correlation as functions of relative time shift in the neighborhood of zero time shift between the two time series under consideration. Figure 4b is for the *unfiltered* EOF-1 time series of GRACE and Altimetry, which are highly correlated (0.69 at zero time shift) as noted above. The AAO Index lags the GRACE time series by a nominal 20 days with a linear correlation coefficient of 0.57 (Figure 4c), and lags Altimetry by 67 days with 0.29 (Figure 4d), both exceeding the 95% confidence level in the present case of the low-pass filtered data series. It is unequivocal to state that the non-seasonal variation of the Argentine Gyre is significantly correlated with AAO in general.

3.3 The ~25-day oscillation

Figure 5 shows the leading CEOF mode of the high-frequency SLV in the Argentine Basin, after the high-pass filtering stated above (Section 2), from GRACE (GRACE CEOF-1, explaining 16% of the total variance) and altimetry (Altimetry CEOF-1, explaining 54% of

the total variance). Figures 5a and 5c show their respective spatial root-mean-square amplitude variability of the modal oscillation. Granting a slight relative shift, the two spatial amplitude patterns agree well in general. So do the corresponding spatial phases given in Figures 5b and 5d, which depict a counterclockwise spin according to the calculated phase (defined to be increasing with time), with the central "amphidrome" point of spin as well as the peak of the *f*/*h* contour located around 42°W, 45°S. Figures S1 and S2 in the Supporting Information presents the 30-day-long reconstructed SLV from GRACE CEOF-1 and Altimetry CEOF-1, showing a dipolar pattern of the counterclockwise spin *within* the Argentine Gyre.

Figure 5e shows that the envelope strength of the dipolar spin, or the "modulation" of the high-frequency SLV amplitude, varies considerably with respect to time. On the other hand, the phase of the spin is quite steady, manifested as the near-secular variation in the form of the (unwrapped) temporal phase in Figure 5f, one estimated at the slope of 1 cycle per 28 days for GRACE (2003/1/5-2012/12/23) and the other at 1 cycle per 23 days for the altimetry (1993/1/1-2015/12/31), both confirming the ~25-day oscillation known to exist from previous studies (Fu et al., 2001; Weatherly, 1993). The discrepancy between the two estimated periods (28 days vs. 23 days) cannot be ascribed to different timespans under study, as the altimetric SLV for the shorter GRACE time-span yields the same results for the temporal phase of 1 cycle per 23 days.

Meanwhile, the correlation between the two temporal amplitude undulations of GRACE CEOF-1 and Altimetry CEOF-1 (shown in Figure 5e) reaches a maximum of 0.55 at zero time shift, far exceeding the 99% confidence level of 0.18 in the presence of our high-pass filtering that reduces the degree of freedom to approximately 120. By the same token as the overall oscillations above, the high correlations found here in both the spatial pattern and

the temporal behavior between GRACE and altimetry ascertain that GRACE is fully capable of catching the ~25-day oscillation within the Argentine Gyre.

The (Morlet) wavelet spectra given in Figures 5g and 5h for the temporal amplitude envelope in Figure 5e (we emphasize that this refers to the amplitude *modulation* envelope of the ~25-days oscillation, not the directly observed or filtered time series) show that the strength of the ~25-day oscillation is itself time-variable in a broad range of timescales. Significant variabilities can be seen in periods of 0.25-0.5 years, within which Fu (2007) suggested an energy exchange between the ~25-day oscillation and the mesoscale eddies. In particular, a prominent annual periodicity indicates that the annual strength of the ~25-day oscillation reaches the peak in the Southern-Hemisphere summer and drops to the trough in the winter. This presumably signifies the seasonal forcing of the mesoscale eddies in the Argentine Basin. The wavelet spectra show that a quasi-biennial modulation from the two datasets are in-phase, albeit almost diminished after 2009 in the GRACE observations.

In parallel, the second CEOF mode of the afore-mentioned ITSG-Grace2016 daily dataset reproduces the ~25-day oscillation, with the following features (see Figure S3 in Supporting Information): a distorted spatial pattern, much smaller amplitude, highly correlated temporal amplitude (0.60 with Altimetry CEOF-1 and 0.36 with GRGS GRACE CEOF-1 both at zero time shift and exceeding 99% confidence level), and a 22-day periodicity. The distortion and weakening of the pattern is possibly owning to the strong filtering scheme applied in the local region during the data generation process.

### 3.4 Comparison with OGCM outputs

Figure 6 shows the leading EOF mode of the non-seasonal SLV from GLORYS2V4 OGCM (explaining 26% of the total variance). The spatial pattern is almost a replication of

Altimetry EOF-1, with a spatially unison up-and-down undulation according to the corresponding time series, which correlates with Altimetry EOF-1 with a correlation coefficient of 0.73 and a time lead of 3 days, and with GRACE EOF-1 with 0.55 at zero time shift (both far exceeding the 99% confidence level of around 0.14 and 0.10). GLORYS2V4 high-frequency SLV captures the ~25-day oscillation as well. The spatial pattern of the leading CEOF mode (see Figures 7 a and 7b) is nearly identical to that of the satellite altimetry (in Figures 5c and 5d), showing a counterclockwise circulating feature centering at around 42°W, 45°S. The period of the leading CEOF mode is about 20 days, shorter than the 23 days resolved by the altimetry, while the temporal amplitude correlates with Altimetry CEOF-1 at the correlation coefficient of 0.24, leading by 18 days in phase and with GRACE CEOF-1 at 0.30, leading by 10 days. Of little surprise as the GLORYS2V4 OGCM assimilates SLV from satellite altimetry, these results do confirm that the eddy-permitting (0.25°) resolution of GLORYS2V4 does allow for the representation of a realistic eddy field as well as the simulation of eddy-driven dynamics related to the Argentine Gyre.

On the other hand, ECCO V4R3 fails to reproduce the characteristics of the Argentine Gyre. The leading EOF mode of non-seasonal SLV from the ECCO V4R3 OGCM shows a uniform vertical oscillation in the Argentine Basin, yet its corresponding time series do not agree with those from GRACE nor with ocean altimetry measurements (see Figure S4 in the Supporting Information). We find no indication of the ~25-day oscillation in the ECCO V4R3 CEOF modes (not shown here), given the fact that the relatively coarse grid of ECCO V4R3 does not allow for the representation of eddy fields, thus the simulation of this eddy-driven ~25-day oscillation is also not realistic. Nonetheless, monthly GRACE mascon solutions have been assimilated into ECCO V4R3 modeling that is evidently unable to capture the sought-after ~25-days variability.

## 4. Discussion and Conclusions

We seek to understand the variability of the Argentine Gyre on temporal and spatial scales hitherto not observed with GRACE data, by analyzing the GRACE TVG data in conjunction with altimetry and OGCM outputs. We aim at (i) the non-seasonal variation of the Argentine Gyre in relation to the AAO using the method of EOF analysis; (ii) the ~25-day oscillation within the Argentine Gyre using the CEOF method.

The strongly correlated signals from the GRACE and altimetry observations have further confirmed the essentially barotropic structure of the non-seasonal variation of the Argentine Gyre. Using bottom pressure-recorder and altimetry measurements, Hughes et al. (2007) asserted that the steric influence constitutes less than 10% of the total signal for the Argentine Gyre. The flow velocities in the region are uniform from surface to bottom, as suggested by oceanographic models (Volkov & Fu, 2008) and comparisons between hydrographic data, satellite altimetry and ARGO profiler measurements (Saraceno et al., 2009). Conversely, the similar spatial distribution as well as time evolution of our leading EOF modes, highly correlated not only in pattern but also matching in absolute amplitude, demonstrate that the GRACE TVG captures the same uniform motion as does the altimetry in a way consistent with the barotropic structure of the Argentine Gyre.

Our EOF analysis reveals that the overall intensity variation of the Argentine Gyre undulates as a standing wave with strength in accordance with the obtained time series that is highly correlated with the AAO in time. Since the mean gyre, upon which the variation is superimposed, is linearly related to the geostrophic velocity, the variation of the Argentine Gyre's velocity field also undulates following the same history in pace with the AAO as does the ACC (see Liau & Chao, 2017).

A spinning dipole at ~25-day periodicity in the form of a propagating wave within the Argentine Gyre is best analyzed by the CEOF method as done here. Displayed in the Supporting Information Figures S1 and S2 are the GRACE CEOF-1 and Altimetry CEOF-1 results of the reconstructed SLV in the Argentine Basin for a duration of 30 days (19 March to 17 April, 2010). The evolving patterns can be characterized as a spatially coherent, counterclockwise spinning dipolar wave with the period of ~25 days. We have obtained different oscillation period estimates for the CEOF leading modes, namely 23-day for altimetry, 28-day for GRGS GRACE, 20-day for GLORYS2V4, and 22-day for ITSG-Grace 2016. At present we have no clear explanation other than numerical uncertainties, for example the numerical unwrapping process of the temporal phase, where abrupt fluctuations abound.

The forcing of the Argentine Gyre's ~25-day oscillation as well as the cause for its temporal variability in strength is still understood inadequately. Fu (2007) provided evidences of interaction between the ~25-day oscillation and the energetic mesoscale variability in the Argentine Basin in the period band of 110-150 days. We suggest that there exist forcing and energy exchanges between the ~25-day oscillation and the main flow on timescale on the order of two years in light of the quasi-biennial modulation found in the ~25-day oscillation that is of opposite phase to the non-seasonal variation (see Figures 5g and 5h and Figures 2d and 2e for comparison). Such interactions are possible by virtue of the Eliassen and Palm theorem as suggested by Tai and Fu (2005), whose mechanism is beyond the scope of the present study. It is however worth noting that the period of the Argentine Gyre's main flow would be about two years assuming its relative vorticity comes only from a curvature effect ($\xi = 4\pi / T$, where the period $T$ is approximately two days as the relatively vorticity change $\xi$ is on the order of $2\times10^{-7}$ $s^{-1}$). While our findings here provide new evidences, further

physical and numerical modeling are required in understanding the dynamics of the Argentine Gyre.

Granted that the GRACE TVG field we analyze is that with the add-back of the inverted-barometer corrected GAB field from the GRACE's background OGCM, we have also conducted the analysis separately for the field without GAB add-back (i.e. using GSM only) and for the GAB itself. Results show that the GSM-only well reproduces the same ~25-day anticyclone oscillation as obtained above in Figure 5 (see Figure S5 in the Supporting Information). However, the ~25-day mode is absent in the GAB field, presumably because its coarse spatial resolution precludes the presence of eddies. This fact implies the inadequacy of the GRACE's background OGCM to capture small spatial-scale variabilities as the Argentine Gyre. By the same token, we have found (not shown) in fact that the atmospheric mass as part of the ocean bottom pressure (GAA dataset), when added back, produces only insignificant differences as far as the EOF and CEOF solutions of the variations of Argentine Gyre are concerned. This is of no surprise as the Argentine Gyre is an oceanographic phenomenon.

In the perspective of the GRACE data application, our study represents a case where the GRACE TVG exhibits higher spatial and temporal resolutions, i.e. finer in spatial-scale and shorter in time-scale, in observing physical phenomenon than typical GRACE applications practiced hitherto. As such, our analysis results for the Argentine Gyre support further applications of GRACE TVG data to observe other similar persistent gyres in the oceans, especially those in the polar regions where in situ records are sparse and altimetry measurements are unavailable or infeasible, and where the spatial resolution is relatively higher, for example for the Ross Gyre and Weddell Gyre in the Southern Ocean. The newly launched GRACE Follow-On mission promises further and finer understanding of these oceanographic phenomena beyond the existing 15-year GRACE observations.

**Acknowledgements**

This work was completed during the first author's visit in the Institute of Earth Sciences of Academia Sinica in Taiwan. We thank the three anonymous reviewers for providing very constructive suggestions in improving the manuscript. We acknowledge the following institutions that provide the online datasets used in this study: GRACE data from GRGS: http://grgs.obs-mip.fr/grace/variable-models-grace-lageos/grace-solutions-release-03; ISTG-Grace 2016 daily solutions: https://www.tugraz.at/institute/ifg/downloads/gravity-field-models/itsg-grace2016/; ocean altimetry data from CMEMS: http://marine.copernicus.eu/services-portfolio/access-to-products/?option=com_csw&view=details&product_id=SEALEVEL_GLO_PHY_L4_REP_OBSERVATIONS_008_047; the AAO Index from Climate Prediction Center of USA National Oceanic and Atmospheric Administration: ftp://ftp.cpc.ncep.noaa.gov/cwlinks/norm.daily.aao.index.b790101.current.ascii; GLORYS2V4 reanalysis model from CMEMS: http://marine.copernicus.eu/services-portfolio/access-to-products/?option=com_csw&view=details&product_id=GLOBAL_REANALYSIS_PHY_001_025; ECCO V4R3 model from JPL: https://ecco.jpl.nasa.gov/products/latest/. All data used in this work are available in the open domain. This work is supported by the Taiwan Ministry of Science and Technology Grants 105-2811-M-001-031 and 106-2116-M-001-013, and by National Nature Science Foundation of China Grants 41474019, 41504014, 41704012.

**References**

Artana, C., Ferrari, R., Koenig, Z., Saraceno, M., Piola, A. R., & Provost, C. (2016), Malvinas Current variability from Argo floats and satellite altimetry, *J. Geophys. Res. Oceans*, 121, 4854–4872, doi:10.1002/2016JC011889.

Bigorre, S. (2005), Topographic effects on wind driven oceanic circulation (Doctoral dissertation). Retrived from: http://diginole.lib.fsu.edu/islandora/object/fsu%3A175937.

Bigorre, S., & Dewar, W. K. (2009), Oceanic time variability near a large scale topographic circulation, *Ocean Modelling*, 29(3), 176-188, doi:10.1016/j.ocemod.2009.04.004.

Cazenave, A., & Nerem, R. S. (2004), Present-day sea level change: Observations and causes, *Rev. Geophys.*, 42, RG3001, doi:10.1029/2003RG000139.

Chao, B. F., O'Connor, W. P., Chang, A. T. C., Hall, D. K., & Foster, J. L. (1987), Snow load effect on the Earth's rotation and gravitational field, 1979-1985, *J. Geophys. Res.*, 92(B9), 9415 9422, doi: 10.1029/JB092iB09p09415.

Chao, B. F. (2005), On inversion for mass distribution from global (time-variable) gravity field, *J. Geodyn.*, 39(3), 223–230, doi:10.1016/j.jog.2004.11.001.

Chao, B. F., Chung, W. Y., Shih, Z. R., & Hsieh, Y.K. (2014), Earth's rotation variations: A wavelet analysis, *Terra Nova*, 26(4), 260-264, doi: 10.1111/ter.12094.

Chelton, D.B., Schlax, M.G., Samelson, R.M. (2011), Global observations of non-linear mesoscale eddies. *Prog. Oceanogr*. 91(2),167–216.

Cheng, M., Ries, J. C., & Tapley, B. D. (2011), Variations of the Earth’s figure axis from satellite laser ranging and GRACE, *J. Geophys. Res.*, 116, B01409, doi:10.1029/2010JB000850.

Cheng, M., & Ries, J. (2017), The unexpected signal in GRACE estimates of C20, *J. Geod.*, 91(8), doi: 10.1007/s00190-016-0995-5.

de Miranda, A. P., Barnier, B., & Dewar, W. K. (1999), On the dynamics of the Zapiola Anticyclone, *J. Geophys. Res.*, 104(C9), 21137–21149, doi:10.1029/1999JC900042.

Dewar, W. K. (1998), Topography and barotropic transport control by bottom friction. *J. Mar. Res.*, 56, 295–328.

Dobslaw, H., Bergmann-Wolf, I., Dill, R., Poropat, L., Thomas, M., Dahle, C., Esselborn, S., König, R., Flechtner, F. (2017), A new high-resolution model of non-tidal atmosphere and ocean mass variability for de-aliasing of satellite gravity observations: AOD1B RL06, *Geophys. J. Int.*, 211(1), 263–269, https://doi.org/10.1093/gji/ggx302

Flood, R. D., & Shor, A. N. (1988), Mud waves in the argentine basin and their relationship to regional bottom circulation patterns. *Deep Sea Res.*, 35(6), 943–971.

Fu, L. -L., Cheng, B., & Qiu, B. (2001), 25-day period large-scale oscillations in the Argentine Basin revealed by the TOPEX/Poseidon altimeter. *J. Phys. Oceanogr.*, 31(2), 506–517.

Fu, L. L. (2007), Interaction of mesoscale variability with large-scale waves in the argentine basin. *J. Phys. Oceanogr.*, 37(3), 787-793, doi:10.1175/JPO2991.1.

Fukumori, I., O. Wang, I. Fenty, G. Forget, P. Heimbach, and R. M. Ponte, 2017: ECCO Version 4 Release 3, http://hdl.handle.net/1721.1/110380, doi:1721.1/110380. Available at ftp://ecco.jpl.nasa.gov/Version4/Release3/doc/v4r3_estimation_synopsis.pdf

García-García, D., Chao, B. F., & Boy, J. P. (2010), Steric and mass-induced sea level variations in the Mediterranean Sea revisited. *J. Geophys. Res.*, 115(C12), doi:10.1029/2009JC005928.

Garzoli, S.L., Piola, A.R., Speich, S., Baringer, M., Goni, G., Donohue, K., … Matano, R.P. (2008), A monitoring system for heat and mass transports in the South Atlantic as a component of the meridional overturning circulation. Workshop Report: Estancia San Ceferino, Buenos Aires, Argentina, 8–10 May 2007, 38 pp, International CLIVAR Project Office, Southampton, UK (available at: http://eprints.soton.ac.uk/50121/)

Hannachi A., Jolliffe, I.T., & Stephenson, D.B. (2007), Review Empirical orthogonal functions and related techniques in atmospheric science: A review. *Int. J. Climatol*. 27(9):1119-1152, doi:10.1002/joc.1499.

Hughes, C. W., Stepanov, V. N., Fu, L.-L., Barnier, B., & Hargreaves, G. W. (2007), Three forms of variability in Argentine Basin ocean bottom pressure. *J. Geophys. Res.*, 112, C01011, doi:10.1029/2006JC003679.

Isern-Fontanet, J., García-Ladona, E., & Font, J. (2003), Identification of marine eddies from altimetry. *J. Atmos. Oceanic Technol.*, 20(5),772–778.

Liau, J. R., & Chao, B. F. (2017), Variation of Antarctic circumpolar current and its intensification in relation to the southern annular mode detected in the time-variable gravity signals by GRACE satellite. *Earth, Planets and Space*, 69, doi:10.1186/s40623-017-0678-3.

Marshall, G. J. (2003), Trends in the southern annular mode from observations and reanalyses. *J. Climate*, 16, 4134-4143.

Mayer-Gürr, T., Behzadpour, S., Ellmer, M., Kvas, A., Klinger, B., Zehentner, N. (2016), ITSG-Grace2016 - Monthly and Daily Gravity Field Solutions from GRACE. GFZ Data Services. http://doi.org/10.5880/icgem.2016.007

Meredith, M. P., et al. (2011), Sustained monitoring of the Southern Ocean at Drake Passage: Past achievements and future priorities, *Rev. Geophys.*, 49, RG4005, doi:10.1029/2010RG000348.

Mo, K. C. (2000), Relationships between Low-Frequency Variability in the Southern Hemisphere and Sea Surface Temperature Anomalies. *J. Climate*, 13, 3599-3610.

Morlet, J., Arens, G., Fourgeau, E., & Glard, D. (1982), Wave propagation and sampling theory, *Geophysics*, 47(2), doi: 10.1190/1.1441328.

Preisendorfer, R.W., & Mobley, C.D. (1988), Principal component analysis in meteorology and oceanography. Elsevier. Amsterdam/New York, ISBN: 0444430148.

Saunders, P. M., & King, B. A. (1995). Bottom currents derived from a shipborne ADCP on WOCE cruise A11 in the South Atlantic. *J. Phys. Oceanogr.*, 25(3), 329-347.

Saraceno, M., Provost, C., Piola, A. R., Bava, J., & Gagliardini, A. (2004), Brazil Malvinas Frontal System as seen from 9 years of advanced very high resolution radiometer data, *J. Geophys. Res.*, 109, C05027, doi:10.1029/2003JC002127.

Saraceno, M., Provost, C., & Zajaczkovski, U. (2009), Long-term variation in the anticyclonic ocean circulation over the Zapiola Rise as observed by satellite altimetry: Evidence of possible collapses. *Deep Sea Res., Part I*, 56(7): 1077-1092.

Saraceno, M., & Provost, C. (2012), On eddy polarity distribution in the southwestern Atlantic. *Deep Sea Res., Part I*, 69(6), 62-69.

Tai, C. K., & Fu, L.-L. (2005), The 25-day-period large-scale oscillations in the argentine basin revisited. *J. Phys. Oceanogr.*, 35, 1473-1479.

Tapley, B. D., Bettadpur, S., Watkins, M., & Reigber, C. (2004), The gravity recovery and climate experiment: Mission overview and early results, *Geophys. Res. Lett.*, 31, L09607, doi:10.1029/2004GL019920.

Venaille, A., Le Sommer, J., Molines, J.-M., & Barnier, B. (2011), Stochastic variability of oceanic flows above topography anomalies, *Geophys. Res. Lett.*, 38, L16611, doi:10.1029/2011GL048401.

Volkov, D. L., & Fu, L.-L. (2008), The role of vorticity fluxes in the dynamics of the Zapiola Anticyclone, *J. Geophys. Res.*, 113, C11015, doi:10.1029/2008JC004841.

Wahr, J., Molenaar, M., & Bryan, F. (1998), Time-variability of the Earth's gravity field: Hydrological and oceanic effects and their possible detection using GRACE, *J. Geophys. Res.*, 103(B12), 30,205–30,230, doi:10.1029/98JB02844.

Weatherly, G. L. (1993). On deep-current and hydrographic observations from a mudwave region and elsewhere in the Argentine Basin. *Deep Sea Research Part II: Topical Studies in Oceanography*, 40(4-5), 939-961.

Weijer, W., Vivier, F., Gille, S. T., & Dijkstra, H. A. (2007), Multiple oscillatory modes of the argentine basin. part i: statistical analysis. *J. Phys. Oceanogr.*, 37(12), 2855-2868, doi:10.1175/2007JPO3527.1.

Willis, J. K., Chambers, D. P., & Nerem, R. S. (2008), Assessing the globally averaged sea level budget on seasonal to interannual timescales, *J. Geophys. Res.*, 113, C06015, doi:10.1029/2007JC004517.

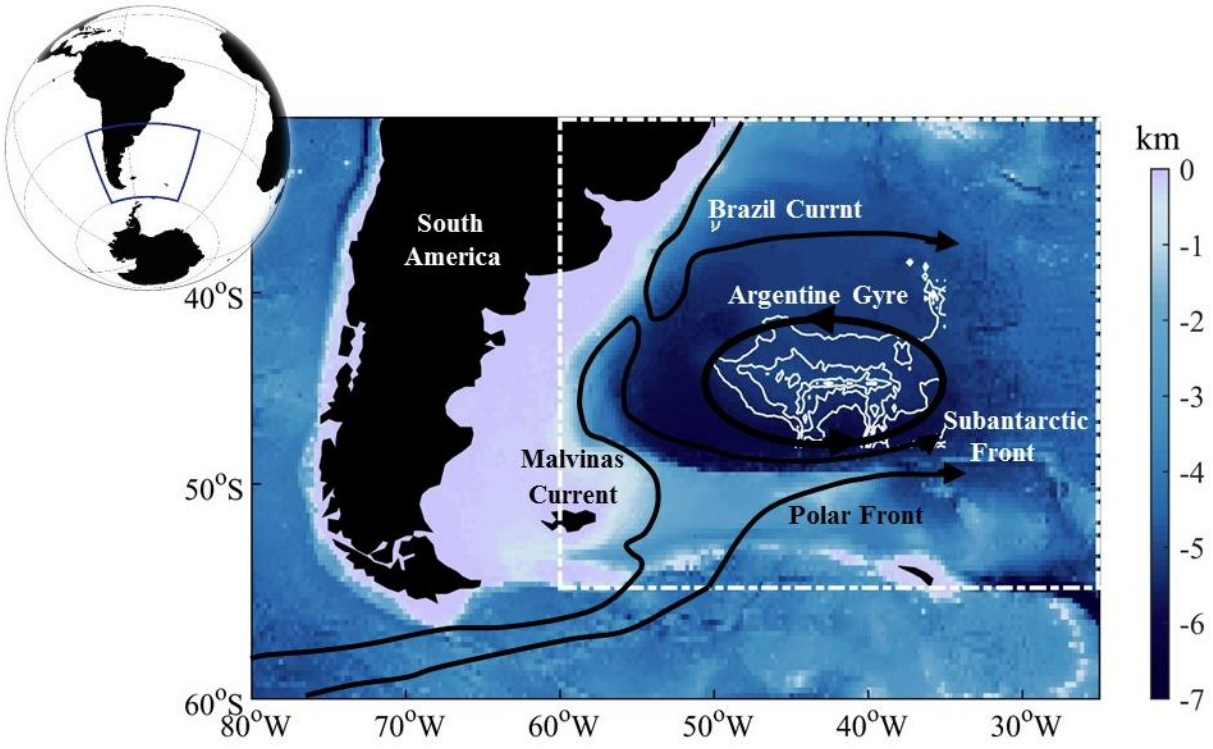


**Figure 1.** The Argentine Basin bathymetry and schematics of the upper-layer circulation in the southwestern Atlantic Ocean (adapted from Artana et al., 2016; Saraceno et al., 2004), showing the Argentine Gyre, Brazil Current, Malvinas Current, Subantarctic Front (also the western edge of the Malvinas return flow) and the Polar Front. The *f*/*h* contours are drawn as thin white lines. The area enclosed by the white dot-dashed lines indicates that shown in later figures.

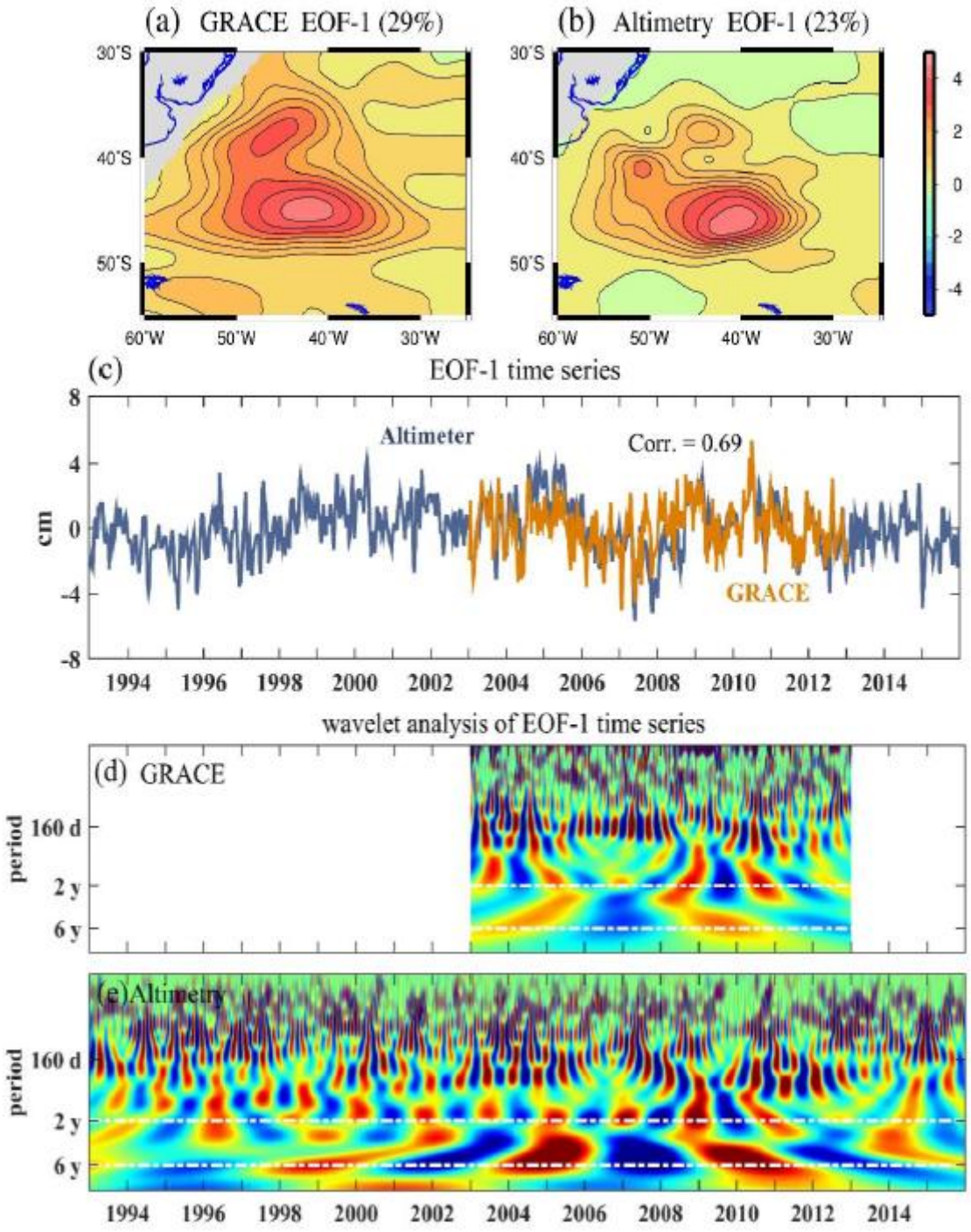


**Figure 2.** The leading EOF modes of the non-seasonal SLV from GRACE and altimetry observations. The normalized spatial pattern of (a) GRACE EOF-1; (b) Altimetry EOF-1. (c) Comparison of the time series of GRACE EOF-1 with Altimetry EOF-1, in unit of cm, with corresponding wavelet spectra in (d) and (e), where color red means peak values, blue trough.

The white dash-dotted lines indicate the periods corresponding to those labeled on the left (see text).

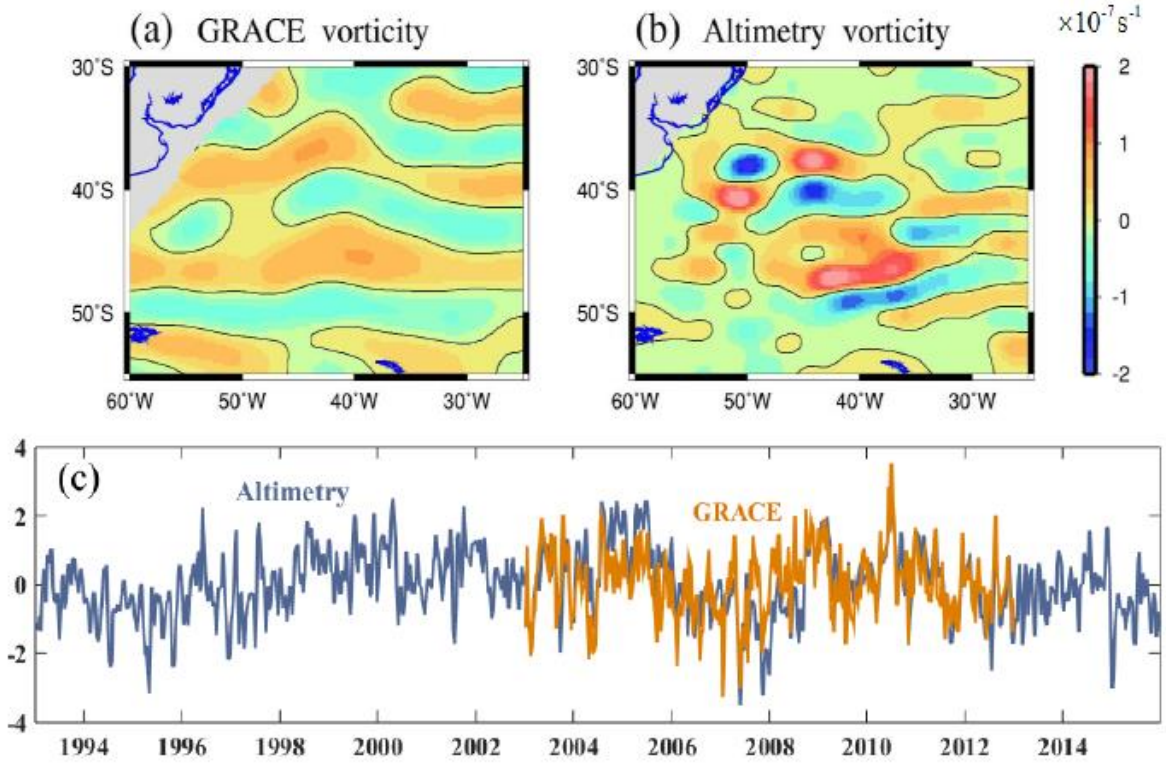


**Figure 3.** Relative vorticity variation $\xi$ in unit of $s^{-1}$ derived from the leading EOF spatial mode: (a) from GRACE EOF-1; (b) from Altimetry EOF-1. (c) The time series are the same as in Figure 2c but normalized here.

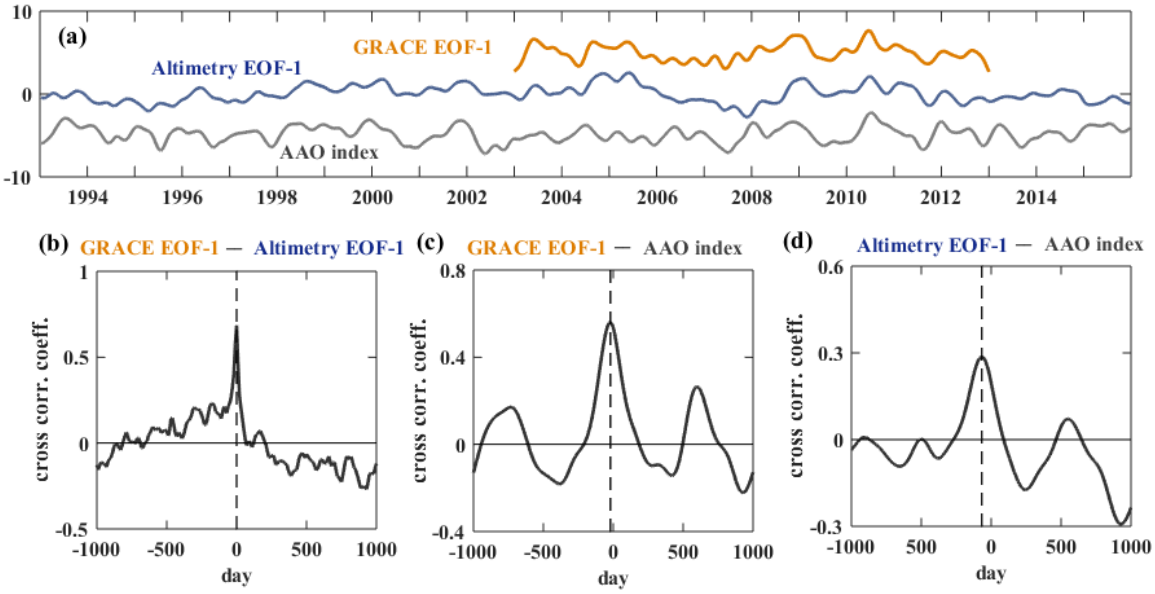


**Figure 4.** (a) Comparison of the time series of GRACE EOF-1 (orange), Altimetry EOF-1 (blue) and AAO Index (gray), all low-pass filtered and normalized to unity standard deviation. Cross correlation functions of relative time shift between the above time series: (b) GRACE EOF-1 and Altimetry EOF-1 (unfiltered); (c) AAO Index and GRACE EOF-1; (d) AAO Index and Altimetry EOF-1.

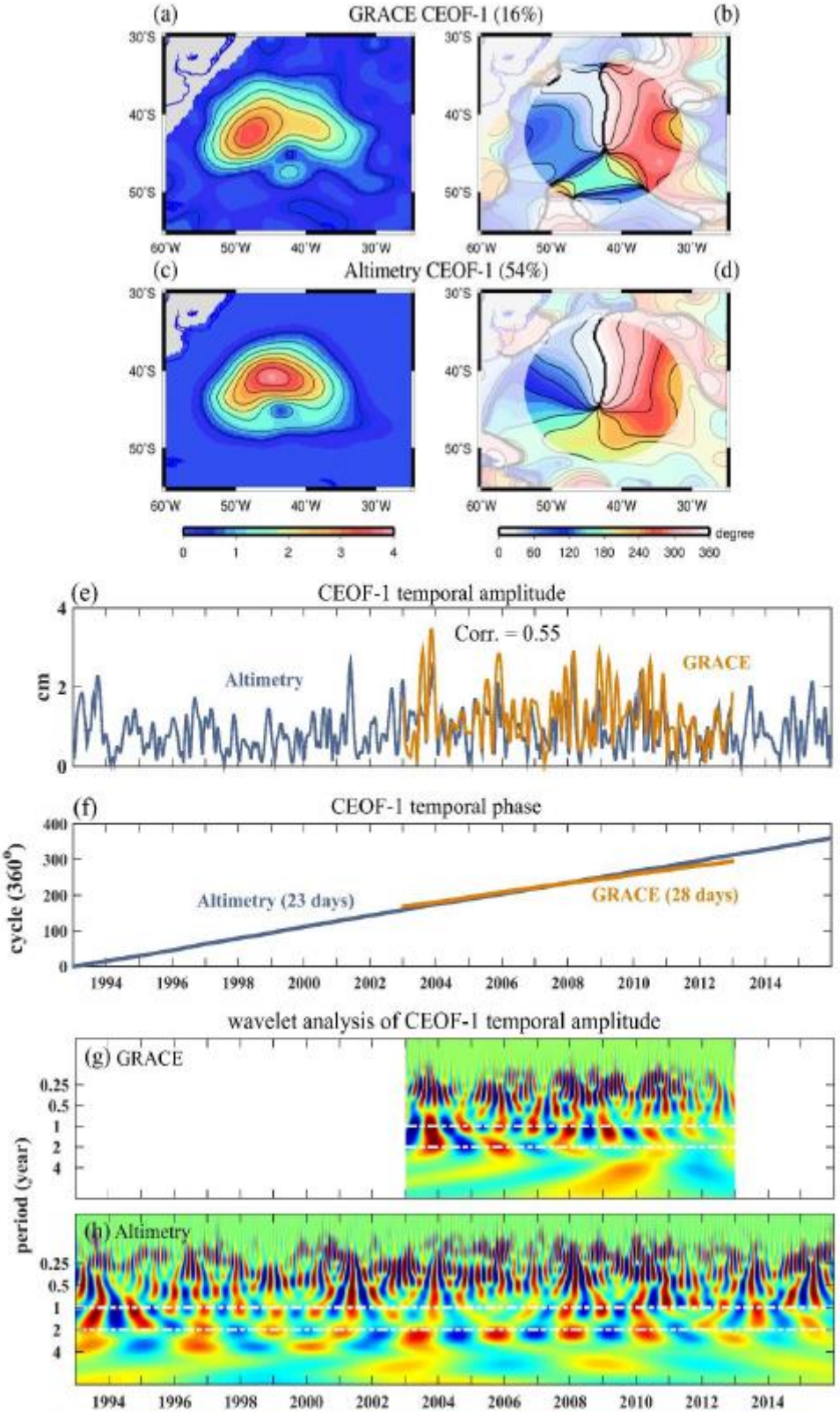


**Figure 5.** The leading CEOF modes of the high-frequency SLV from GRACE and altimetry measurements: GRACE CEOF-1's (a) normalized spatial amplitude; (b) spatial phase in

degrees; and Altimetry CEOF-1's (c) normalized spatial amplitude and (d) spatial phase in degrees (lighter shade indicates regions of less well determined). (e) Comparison of the temporal amplitude of GRACE CEOF-1 and Altimetry CEOF-1, in unit of cm. (f) Comparison of the unwrapped temporal phase of GRACE CEOF-1 and Altimetry CEOF-1, in unit of cycle (360°). Wavelet spectrum of the temporal amplitude of (g) GRACE CEOF-1 and (h) Altimetry CEOF-1, where color red means peak values and blue trough; the white dash-dotted lines indicate the periods corresponding to those labeled on the left.

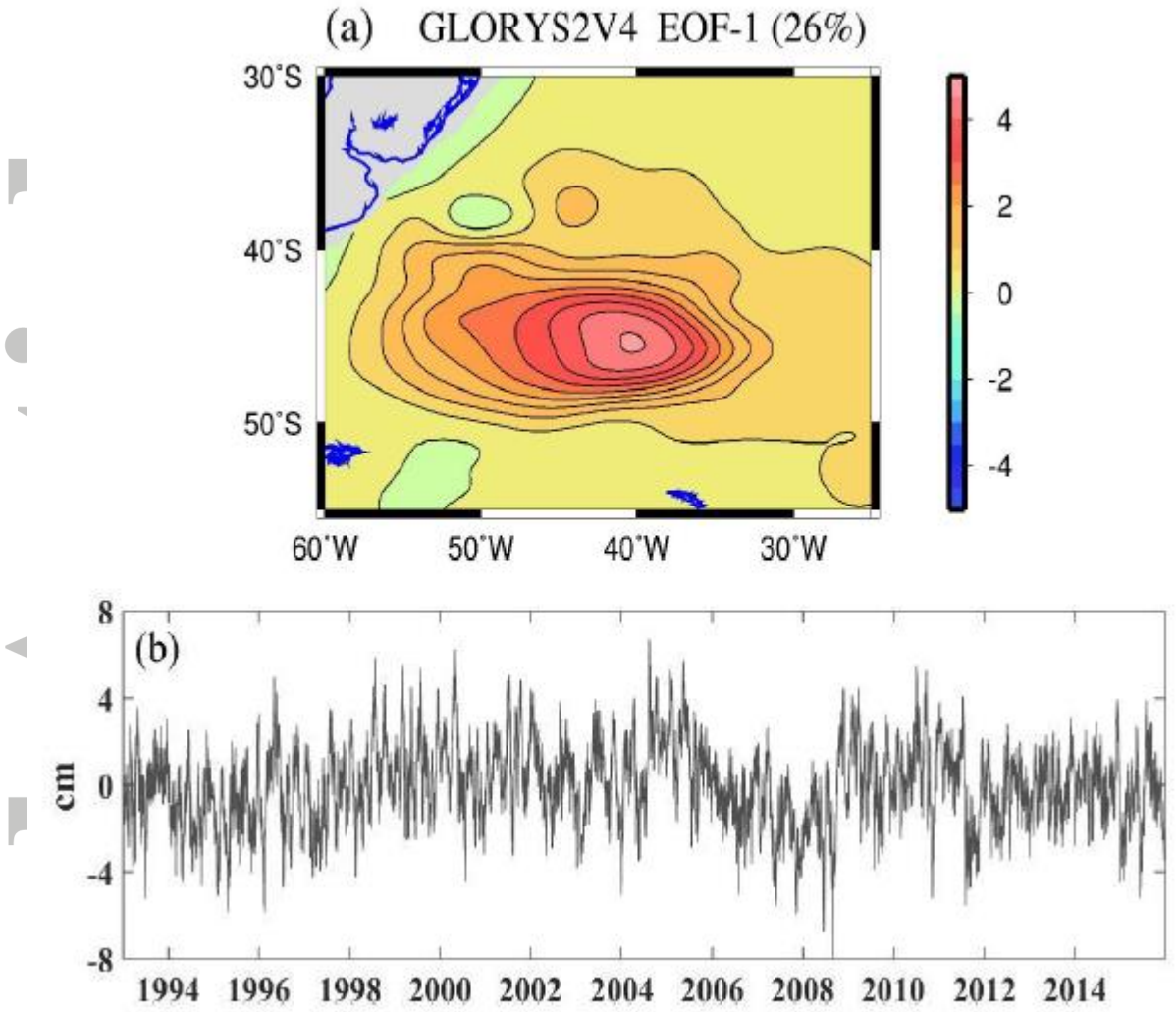


**Figure 6.** The leading EOF mode of the non-seasonal SLV from GLORYS2V4 OGCM: (a) normalized spatial pattern and (b) time series in unit of cm.

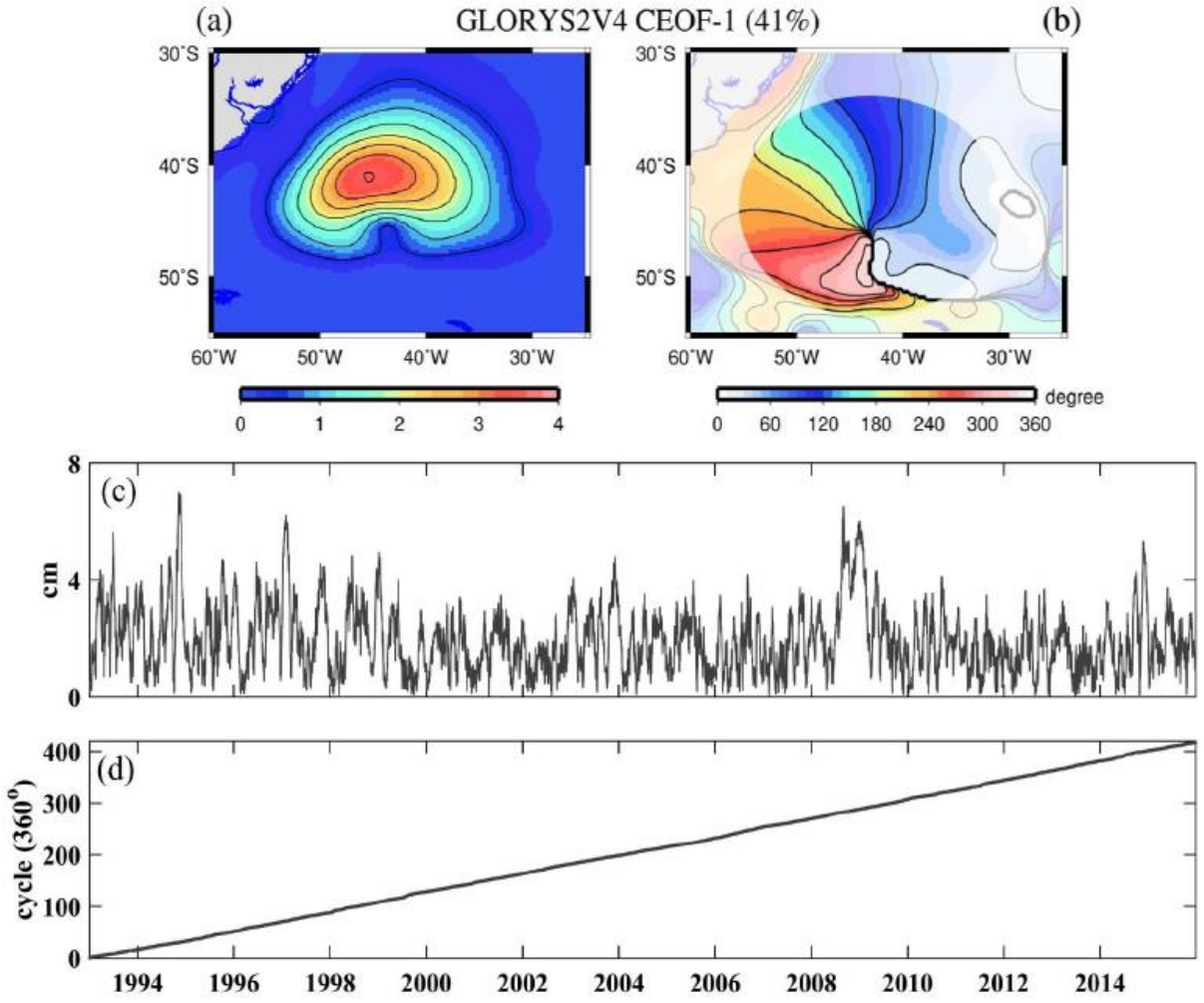


**Figure 7.** The leading CEOF mode of the high-frequency SLV from GLORYS2V4 OGCM: (a) normalized spatial amplitude; (b) spatial phase in degrees (lighter shade indicates regions of less well determined); (c) temporal amplitude in unit of cm; (d) unwrapped temporal phase in unit of cycle (360°).